Journal of Solid State Chemistry 184 (2011) 1–6

Contents lists available at ScienceDirect

Journal of Solid State Chemistry

journal homepage: www.elsevier.com/locate/jssc

Rapid crystallization and morphological adjustment of zeolite ZSM-5 in nonionic emulsions

Ying Zhang [a,b,*], Chao Jin [b,c]

[a] The State Key Laboratory of Heavy Oil Processing, China University of Petroleum, Beijing 102249, PR China
[b] Department of Materials Science and Engineering, China University of Petroleum, 18 Fuxue Road, Changping District, Beijing 102249, PR China
[c] Research Institute of Petroleum Processing, Beijing 100083, China

ARTICLE INFO

Article history:
Received 4 July 2010
Received in revised form
14 September 2010
Accepted 11 October 2010
Available online 19 October 2010

Keywords:
Nonionic emulsion
Zeolite ZSM-5
Crystallization
Morphology

ABSTRACT

Zeolite ZSM-5 was synthesized for the first time in a nonionic emulsion composed of polyoxyethylated alkylphenol, butanol, cyclohexane and tetraethylammonium hydroxide (TEAOH)-containing zeolite synthesis mixture. The crystallization kinetics in the emulsion was investigated and the ZSM-5 product was characterized in detail by XRD, SEM, FT-IR, TG, N_2 adsorption and CHN analysis techniques. Compared with the conventionally hydrothermal synthesis with the same structure directing agent TEAOH, the emulsion system allows rapid crystallization of ZSM-5. The ZSM-5 product exhibits unusual agglomerated structure and possesses larger specific surface area. The FT-IR, TG results plus CHN analysis show the encapsulation of a trace of emulsion components in the emulsion ZSM-5. Control experiments show the emulsion system exerts the crystallization induction and morphological adjustment effects mainly during the aging period. The effects are tentatively attributed to the confined space domains, surfactant–water interaction as well as surfactant-growing crystals interaction existing in the emulsion.

1. Introduction

Zeolites, widely used as catalysts, adsorbents and ion exchangers in chemical process industries, are usually crystallized from aluminosilicate gels heated in oven from several minutes to days. Short crystallization time has always been pursued from the commercial viewpoint since it is associated with high synthesis efficiency, low energy consumption and thus low production cost. Till date, many ways have been developed to shorten zeolite crystallization time, including careful choice of silica source [1], fine adjustment of initial gel composition [2], controlling crystallization temperature [3,4], adding seeds [5–8], aging before crystallization [9,10] and using microwave dielectric heating [11]. For example, through acid-catalyzed hydrolysis of tetraethyl orthosilicate, MCM-22 was synthesized at 158 °C under static conditions with a crystallization time of only 3 days [1]. ZSM-5 was obtained after several hours using optimized synthesis parameters and a relatively fast heating ramp rate [2]. A two-step synthesis procedure, where the gel was first heated at 160 °C for 2 h and after that the temperature was raised to 210 °C, allowed synthesizing ZSM-5 within 7 h [3]. Under high pressure (40–60 atm) and high temperature (230–250 °C) in various solvents, 4–6 h syntheses of ZSM-5 were achieved [4]. Adding seeds as an effective and general way to quicken zeolite crystallization process is frequently used although it is discovered in early days. The common zeolites including BEA, LTA, FAU, MOR and MFI have been synthesized via the seeding method. Various forms of seeds have been used to induce zeolite growth, such as normal zeolite crystals [5], crystals after tribochemical activation [6], in-situ generated seeds [7] and synthesis gels [8]. Aging under ambient conditions before crystallization can strongly influence zeolite crystallization since structural rearrangements occur during the aging that lead to the formation of zeolite nuclei [9]. Valtchev et al. [10] synthesized MFI-type nanoparticles via long aging of the initial mixture combined with a very high heating rate. For the synthesis system aged for 60 days at 25 °C, a substantial increase was observed in the crystallization rate, i.e., the first crystals were found after 15 min of hydrothermal synthesis at 170 °C. Using microwave dielectric heating, a significant shortening of zeolite crystallization can be achieved. Cundy et al. [11] have synthesized ZSM-5 for 3 min using the synergistic effect of microwave heating and zeolite seeds.

Recently, the crystallization of zeolites or zeolite analogs in microemulsions has been reported [12–26]. The early example was the growth of microporous zincophosphate in reverse micelles using bis(2-ethylhexyl)sulfosuccinate(AOT) as surfactant, which showed that reverse micelles media can serve as a convenient means of controlling morphology of growing crystals [12–15]. Later on, a bicontinuous microemulsion system containing AOT was used to synthesize uniform silicalite-1 aggregates composed of small crystal

* Corresponding author at: Department of Materials Science and Engineering, China University of Petroleum, 18 Fuxue Road, Changping District, Beijing 102249, PR China. Fax: +86 10 89733200.
E-mail address: yingzh1977@163.com (Y. Zhang).

0022-4596/$ - see front matter © 2010 Elsevier Inc. All rights reserved.
doi:10.1016/j.jssc.2010.10.012

plates grown from a common crystal center [16]. Cationic microemulsions have also been used to adjust the crystal morphology. For example, Yates et al. [17–19] obtained novel AlPO4-5 fibers with AFI structure type in a cationic microemulsion containing cetylpyridium chloride. They also adjusted silicalite-1 morphology from coffin-shaped to novel rod-shaped and to irregular-shaped nanoparticles by varying the microemulsion composition of water-in-oil microemulsions containing cetyltrimethylammonium bromide [20]. Silicalite-1 particles with rich morphology were also synthesized, respectively, in anionic, cationic and nonionic microemulsions by Shantz et al. [21–25]. For the first time they reported nonionic-microemulsion mediated growth of zeolite A and found the microemulsion can induce rapid zeolite growth [26]. Relative to the aforementioned morphology and size control effects, the crystallization induction effects of microemulsions on zeolite synthesis are rarely known. Moreover, almost all the microemulsion-mediated or emulsion-mediated zeolite growth is limited to zeolite A and silicalite-1.

Zeolite ZSM-5 possesses a three-dimensional network composed of straight channels of 0.54 nm × 0.56 nm, intersecting with sinusoidal channels of 0.53 nm × 0.55 nm [27]. It has been widely used as catalysts and selective adsorbents in the petrochemical industry owing to their high thermal stability, intrinsic acidity, high surface area and well-defined porosity. Here we reported for the first time the synthesis of ZSM-5 in a nonionic emulsion system composed of polyoxyethylated alkylphenol (OP-10), butanol, cyclohexane and zeolite synthesis mixture. The crystallization process of ZSM-5 in the nonionic emulsion was investigated and the ZSM-5 sample was characterized in detail by XRD, SEM, FT-IR, TG, N_2 adsorption and CHN analysis techniques. For comparison, the conventional ZSM-5 synthesis was also carried out to find out the effects of emulsions. Finally, several control experiments were designed to ascertain the effects of the nonionic emulsions and some speculations on crystallization mechanism were tentatively proposed.

2. Experimental

2.1. Synthesis of the conventional zeolite ZSM-5

First, a clear solution was prepared by mixing distilled water, TEAOH (25%, Qingdao Haiyang Chemical Product Limited Company) and aluminum isopropoxide (Al_2O_3 ≥45%, Tianjin Jinke Fine Chemical Product Limited Liability Company). Second, silica sol (40%, Qingdao Haiyang Chemical Product Limited Company) was added to the clear solution under stirring. The final zeolite synthesis mixture had the molar composition of $9TEAOH:0.25Al_2O_3:25SiO_2:490H_2O$. After stirring for 60 min, the mixture was transferred to Teflon-lined stainless steel autoclaves, aged at 70 °C for 12 h and then crystallized at 175 °C for 0–60 h. After finishing crystallization, the solid product was filtered, washed with distilled water, dried at 100 °C overnight and if necessary, calcined at 550 °C for 5 h.

2.2. Synthesis of the emulsion zeolite ZSM-5

The nonionic emulsion was prepared by mixing polyoxyethylated alkylphenol (OP-10, Tianjin Yingda Chemical Reagent Factory), butanol (99.0%, Beijing Beihua Fine Chemical Product Limited Liability Company), cyclohexane (99.5%, Beijing Beihua Fine Chemical Product Limited Liability Company) and the conventional zeolite ZSM-5 synthesis mixture (see Section 2.1). The emulsion composition is OP-10:butanol:cyclohexane:zeolite synthesis mixture to 27:13:40:20. After stirring for 60 min, the emulsion system was transferred to Teflon-lined stainless steel autoclaves. The subsequent heating conditions and product treatment are the same as those used in the conventional ZSM-5 synthesis.

2.3. Characterization

X-ray diffraction (XRD) measurements were performed using a Rigaku D/MAX-2500 X-ray diffractometer with Cu$K\alpha$ radiation. Samples were analyzed over a range of 5–35° 2θ using a step scan mode with a step rate of 4°/min. Scanning electron microscopy (SEM) measurements were performed using a CAMBRIDGE S-360 microscope. The FT-IR spectra of synthesized samples were measured as KBr wafers with DIGLAB FTS-3000 spectrometer over a range of 400–4000 cm^{-1}. Nitrogen adsorption experiments of calcined samples were performed on an ASAP 2020 micropore analyzer. TG measurements were performed using a STA 409PC thermogravimetry and differential thermal analysis and the temperature ranged from 25 to 800 °C. LECO CS-600 elemental analyzer was applied to determine the carbon and nitrogen content in the synthesized ZSM-5 sample.

3. Results and discussion

3.1. Kinetic studies on the nonionic emulsion and conventional synthesis of zeolite ZSM-5

Fig. 1 displays the X-ray diffraction (XRD) patterns of the samples synthesized at different crystallization times and thereby calculated kinetics curves in the conventional and nonionic emulsion systems. For the conventional synthesis, zeolite ZSM-5 began to form at about 36 h and thereafter grew with prolonging crystallization time. The crystallization was completed at 53 h and longer crystallization time resulted in lower intensity. Notably, in comparison with the conventional ZSM-5 synthesis using tetrapropyl ammonium (TPA) cations as structure-directing agents, the present synthesis employing TEA cations shows longer induction period due to the stronger hydrophilic interaction of TEA with water molecules [28]. For the nonionic emulsion synthesis, zeolite ZSM-5 with the relative crystallinity of about 40% formed in 24 h and the crystallization was accomplished at 48 h. The curves of the crystallization kinetics for the emulsion and conventional ZSM-5 synthesis are of the same character but differ in the duration of the nucleation period and the crystallization rate. The induction period substantially decreased for the emulsion sample, followed by an increase in the crystallization rate. As a result, the crystallinity of the emulsion samples is much higher than that of the conventional samples at the same crystallization times. The emulsion may induce the formation of a large number of nuclei and ensure fast crystallization. This phenomenon was also observed by our previous nonionic emulsion synthesis of zeolite Y [29].

3.2. Morphological and pore structural features of the ZSM-5 samples

Based on the kinetics curves of the ZSM-5 samples, the emulsion sample crystallized at 175 °C for 48 h and the conventional sample for 53 h have the best crystallinity and chosen as typical ZSM-5 samples for comparison. SEM images given in Fig. 2 show the conventional sample exhibits dispersed ordinary coffin-shaped particles with the mean particle size of about 5 μm. The emulsion sample also shows coffin-shaped profile, but the particles have smaller size of about 3 μm and each large particle is composed of small particles. Similar aggregate morphology has also been observed in the emulsion or microemulsion-mediated syntheses of silicalite-1 [16], zeolite A [26] and zeolite Y [29].

The pore structure parameters listed in Table 1 calculated from nitrogen adsorption isotherms show the two ZSM-5 samples have

similar pore volumes, but the emulsion ZSM-5 sample has larger BET surface area of 371.04 m^2/g and external surface area of 178.60 m^2/g, compared to the corresponding values of 255.70 and 103.11 m^2/g for the conventional ZSM-5 sample. These results may suggest most of the emulsion components are not encapsulated in the ZSM-5 particles, otherwise the removal of the emulsion components

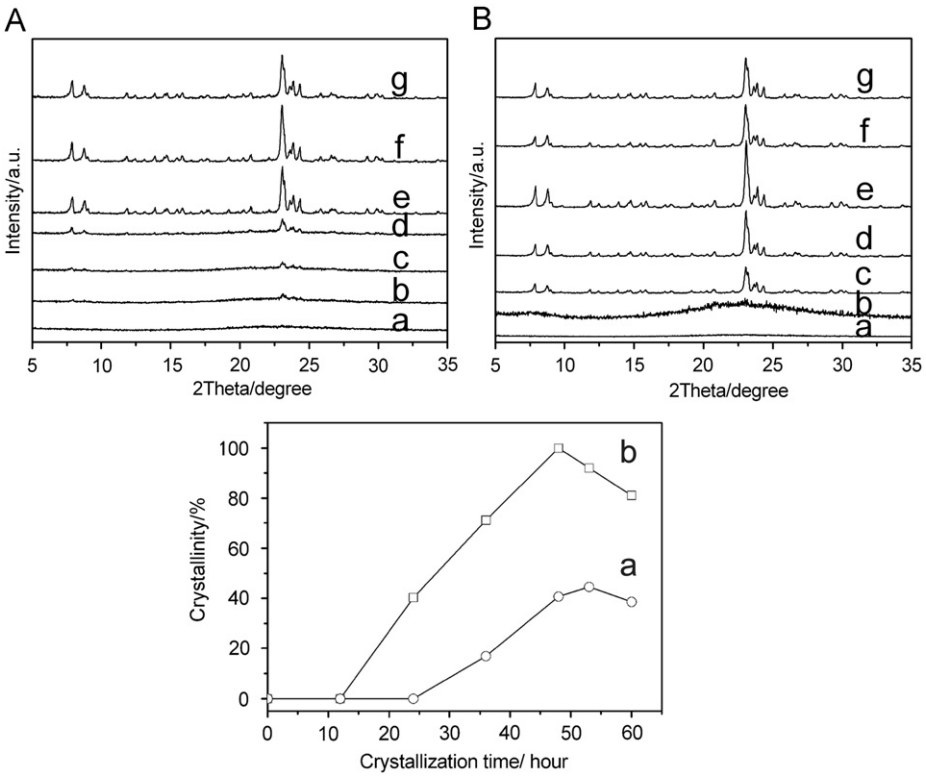

Fig. 1. X-ray diffraction patterns and kinetics curves of the ZSM-5 samples crystallized (A) in the conventional system and (B) in the emulsion system at 175 °C for (a) 0 h, (b) 12 h, (c) 24 h, (d) 36 h, (e) 48 h, (f) 53 h and (g) 60 h.

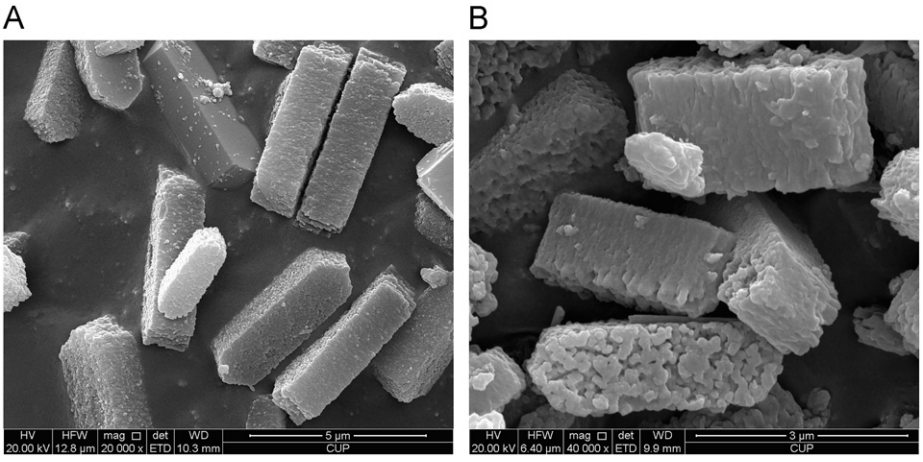

Fig. 2. SEM images of the ZSM-5 samples crystallized (A) at 175 °C for 53 h in the conventional system and (B) at 175 °C for 48 h in the emulsion system.

Table 1
Pore structure parameters, weight losses and carbon and nitrogen content of the ZSM-5 samples synthesized in (A) the conventional, (B) emulsion and (C) NaCl added emulsion systems.

Samples	S_{BET} (m^2g^{-1})	*t*-Plot external surface area (m^2g^{-1})	Total pore volume ($cm^3\,g^{-1}$)	BJH cumulative pore volume ($cm^3\,g^{-1}$)	*t*-Plot micropore volume ($cm^3\,g^{-1}$)	Weight loss (%)	Carbon content (%)	Nitrogen content (%)
A	255.70	103.11	0.18	0.10	0.07	8.55	6.02	1.44
B	371.04	178.60	0.21	0.09	0.09	9.00	6.08	1.35
C	370.95	169.32	0.21	0.08	0.09	8.91	–	–

through calcination would produce additional pore aperture and increase total pore volume. Apparently, the increase of the BET surface area for the emulsion ZSM-5 is mainly due to the increase of the external surface area, which is attributed to the aggregated small particles comprising the large coffin-shaped particles.

In order to confirm if there are emulsion components encapsulated in the emulsion ZSM-5, the synthesized emulsion and conventional ZSM-5 samples are characterized by FT-IR, TG and CHN analysis. It is found that both samples have almost the same FT-IR spectra and it is hard to discern the absorption bands corresponding to the emulsion components, i.e., OP-10, butanol and cyclohexane, due to the presence of TEAOH in both samples.

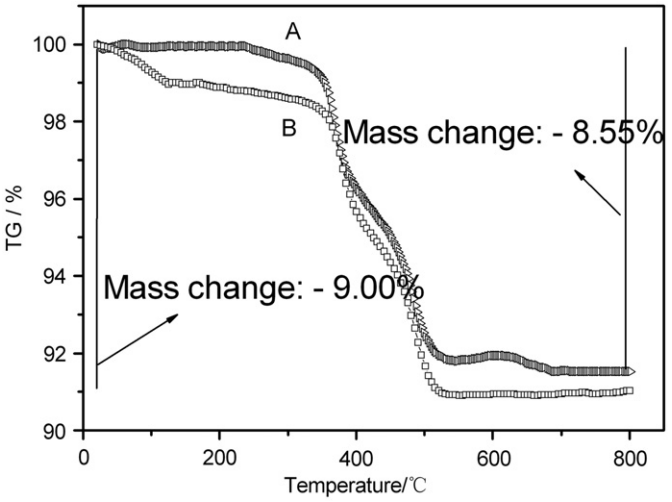

Fig. 3. TG curves of the ZSM-5 samples crystallized (A) at 175 °C for 53 h in the conventional system and (B) at 175 °C for 48 h in the emulsion system.

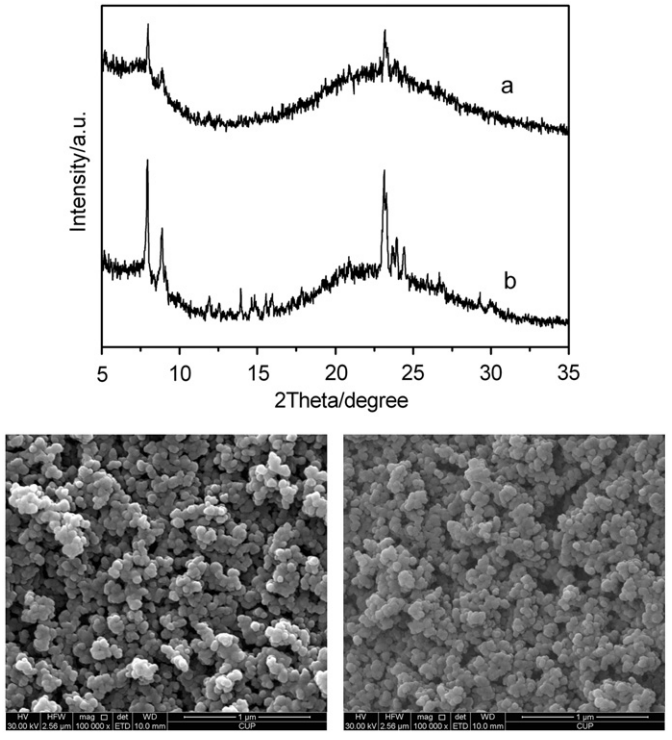

Fig. 4. XRD patterns and SEM images of the ZSM-5 samples directly crystallized without aging (a) at 175 °C for 53 h in the conventional system and (b) at 175 °C for 48 h in the emulsion system.

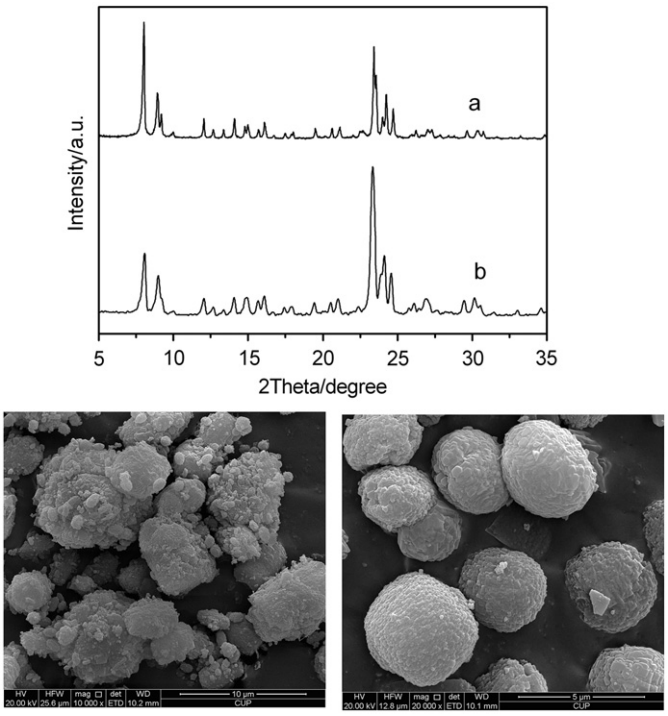

Fig. 5. XRD patterns and SEM images of the ZSM-5 samples synthesized from (a) the conventional synthesis system and (b) the nonionic emulsion system in the presence of NaCl.

Therefore, the two samples are further characterized by thermal analysis and the TG curves are shown in Fig. 3. For the conventional ZSM-5, the initial weight loss of 1.35% before 350 °C is due to the loss of water molecules and the second step of weight loss of 7.20% corresponds to the decomposition of the template TEAOH molecules. However, the emulsion sample shows three steps of weight losses of 1.13%, 0.75%, 7.12%, respectively, in the ranges of 20–150, 150–350 and 350–550 °C, likely correspond to the decomposition of water/butanol/hexane, OP-10 and TEAOH. The total weight loss of the emulsion sample is 9.0%, which is larger than 8.55% for the conventional sample (Table 1). These results indicate the encapsulation of a trace of emulsion components and the decrease in the amount of TEAOH molecules in the emulsion ZSM-5 product, which are confirmed by CHN analysis results in Table 1. The nitrogen content of the emulsion sample is lower than that of the conventional sample, but the carbon content is higher due to the introduction of emulsion components.

3.3. Control experiments to recognize the effects of nonionic emulsions

Aging before crystallization was employed in this work both for the conventional and emulsion syntheses since aging is well known as an effective way to increase the crystallization rate of MFI-type crystals. To ascertain the effect of aging on the crystallization process in the emulsion system, emulsion and conventional syntheses were performed directly at 175 °C without aging. As seen from the XRD patterns shown in Fig. 4, both samples show very weak XRD diffraction peaks compared with the products from the corresponding syntheses with aging (Fig. 1), indicating aging has a pronounced effect on the quick crystallization of zeolite ZSM-5. Further comparison of both the samples finds the emulsion sample possesses XRD diffraction peaks with slightly higher intensities, but the intensity difference is not as pronounced as that observed in the syntheses

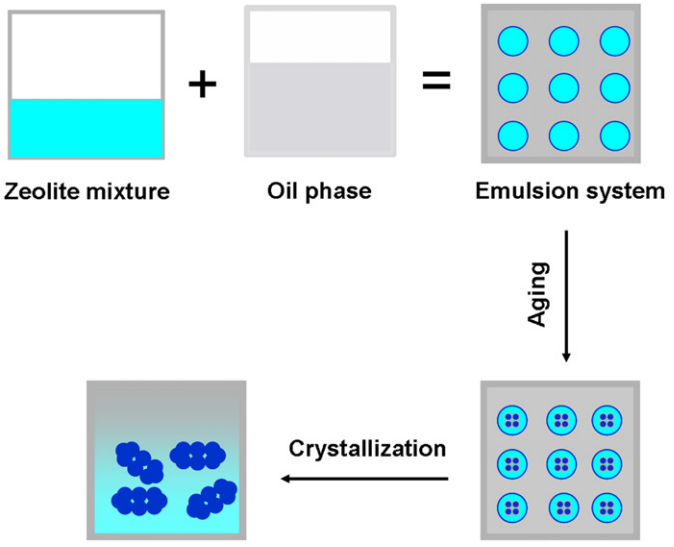

Fig. 6. Schematic illustration of zeolite formation process in the emulsion system.

with aging (Fig. 1). SEM images (Fig. 4) show both samples have almost the same spheric morphology, clearly different from the coffin-shaped particles produced in the syntheses with aging. The above results show the emulsion components exert both crystallization induction and morphological adjustment effects mainly during aging period although they slightly stimulate the crystal growth. The effects of emulsion components during aging are further confirmed by control experiments applying ultrasonic techniques. Emulsion is known to be kinetically stable dispersions of oil and water domains stabilized by the interfacial film of surface active agents. Ultrasonic treatment of the initial mixture is used to separate the oil and water phase and thus destroy the emulsion system. As a result, the product from the ultrasonic treated mixture has almost the same crystallinity and morphology as the conventional sample.

To further investigate the effect of the emulsion, sodium chloride electrolyte was added to both the conventional and emulsion systems while the synthesis conditions are the same as those for the typical ZSM-5 samples. The XRD and SEM results of both samples are shown in Fig. 5. XRD patterns show the emulsion sample with sodium chloride has higher crystallinity than that of the conventional sample with sodium chloride. SEM images show the addition of sodium chloride leads to obvious morphology change from coffin-shaped to elliptical particles, but the emulsion sample has uniform shape with smooth surface. The pore parameters and weight loss are listed in Table 1, which are similar to the data of the emulsion sample without sodium chloride. These results show the emulsion system influences particle morphology in a different way when sodium chloride is added, but the specific details are still unclear.

3.4. Speculation on the effects of emulsion components

For the emulsion synthesis herein, the emulsion mixture composed of OP-10, butanol, cyclohexane and TEA-containing zeolite synthesis mixture, is first aged at 70 °C and then crystallized at 175 °C. The emulsion is proved to work mainly during the aging period since the emulsion is stable only during aging period and high temperature crystallization process will destroy it. Similar to our previous synthesis of zeolite Y in the nonionic emulsion [29], during aging dispersed confined space domains with high concentration of zeolite precursors are first generated. The high concentration greatly stimulates zeolite nucleation and quickens the whole crystallization rate. Additionally, the hydrophilic action of nonionic surfactants may also contribute to the quick crystallization because it can weaken the hydration of TEA cations to facilitate the replacement of the water molecules around TEA by silica oligomers, which is suggested to be a part of the lowest-energy pathway for zeolite formation [30]. On the other hand, the confined space domains formed during aging as well as the surfactant-growing crystals interaction during crystallization are crucial for the formation of small particles and their assembly into coffin-shaped large particles. Due to the separation of oil and water phase under the high temperature crystallization process, most of the surfactants are transferred into the oil phase. This may be the reason why a trace of emulsion components is encapsulated in the emulsion ZSM-5. The formation process in the emulsion system is schematically illustrated in Fig. 6.

4. Conclusions

Zeolite ZSM-5 was first synthesized in a nonionic emulsion system containing polyoxyethylated alkylphenol surfactants and then characterized using XRD, SEM, FT-IR, TG, N_2 adsorption and CHN analysis techniques. It is found that the emulsion systems can not only shorten the induction period but also change particle morphology. Several control experiments are designed to ascertain the effects of the nonionic emulsions and the emulsions are speculated to exert the effects via confined space domains, surfactant–water interaction as well as surfactant-growing crystals interaction. This work demonstrates emulsion synthesis system is applicable for the rapid crystallization and morphological adjustment of aluminosilicate zeolites involving structure-directing agents such as TEA cations.

Acknowledgments

This work was supported by the National Natural Science Foundation of China (Grant no. 20606038) and Beijing Natural Science Foundation (Grant no. 2093043).

References

[1] Y.J. Wu, X.Q. Ren, Y.D. Lu, J. Wang, Mater. Lett. 62 (2008) 317–319.
[2] S. Ahmed, M.Z. El-Faer, M.M. Abdillahi, M.A.B. Siddiqui, S.A.I. Barri, Zeolites 17 (1996) 373–380.
[3] T. Inui, M.L. Occelli, H. Robson (Eds.), ACS Symposium Series, American Chemical Society, Washington, DC, 1989.
[4] S.J. Kulkarni, P. Srinivasu, N. Narender, K.V. Raghavan, Catal. Commun. 3 (2002) 113–117.
[5] J. Warzywoda, R.D. Edelman, R.W. Thompson, Zeolites 11 (1991) 318–324.
[6] V. Valtchev, S. Mintova, V. Dimov, A. Toneva, D. Radev, Zeolites 15 (1995) 193–197.
[7] M. Shibata, J. Gérard, Z. Gabelica, Micropor. Mater. 12 (1997) 141–148.
[8] P.K. Dutta, J. Bronic, Zeolites 14 (1994) 250–255.
[9] G.A. Tompsett, W.C. Conner, K.S. Yngvesson, Chem. Phys. Chem. 7 (2006) 296–319.
[10] V.P. Valtchev, A. Faust, J. Lézervant, Micropor. Mesopor. Mater. 68 (2004) 91–95.
[11] C.S. Cundy, R.J. Plaisted, J.P. Zhao, Chem. Commun. (1998) 1465–1466.
[12] M.J. Castagnola, P.K. Dutta, Micropor. Mesopor. Mater. 20 (1998) 149–159.
[13] P.K. Dutta, M. Jakupca, K.S. Reddy, L. Salvati, Nature 374 (1995) 44–46.
[14] K.S.N. Reddy, L.M. Salvati, P.K. Dutta, J. Phys. Chem. 100 (1996) 9870–9880.
[15] R. Singh, P.K. Dutta, Langmuir 16 (2000) 4148–4153.
[16] A. Manna, B.D. Kulkarni, R.K. Ahedi, A.N. Kotasthane, J. Colloid Interface Sci. 213 (1999) 405–411.
[17] M.Z. Yates, K.C. Ott, E.R. Birnbaum, Angew. Chem. Int. Ed. 41 (2002) 476–478.
[18] J.C. Lin, J.T. Dipre, M.Z. Yates, Chem. Mater. 15 (2003) 2764–2773.
[19] J.C. Lin, J.T. Dipre, M.Z. Yates, Langmuir 20 (2004) 1039–1042.
[20] J.C. Lin, M.Z. Yates, Langmuir 21 (2005) 2117–2120.
[21] S. Lee, D.F. Shantz, Chem. Commun. 6 (2004) 680–681.
[22] S. Lee, D.F. Shantz, Chem. Mater. 17 (2005) 409–417.
[23] S. Lee, D.F. Shantz, Micropor. Mesopor. Mater. 86 (2005) 268–276.
[24] S. Axnanda, D.F. Shantz, Micropor. Mesopor. Mater. 84 (2005) 236–246.
[25] S. Lee, D.F. Shantz, Langmuir 21 (2005) 12031–12036.
[26] C.S. Carr, D.F. Shantz, Micropor. Mesopor. Mater. 85 (2005) 284–292.

[27] M.A. Salomón, J. Coronas, M. Menéndez, J. Santamaría, Chem. Commun. 1 (1998) 125–126.
[28] D.S. Kim, J.S. Chang, J.S. Hwang, S.E. Park, J.M. Kim, Micropor. Mesopor. Mater. 68 (2004) 77–82.
[29] Y. Zhang, C. Jin, Y.G. Shen, Y. Cao, W. Gao, L.S. Cui, J. Sol–Gel Sci. Technol. 54 (2010) 212–219.
[30] A.V. Goretsky, L.W. Beck, S.I. Zones, M.E. Davis, Micropor. Mesopor. Mater. 28 (1999) 387–393.